

# INTERACTIVE STEREO RENDERING FOR NON-PLANAR PROJECTIONS OF 3D VIRTUAL ENVIRONMENTS

*With a Comparison of Image- and Geometry-based Approaches*

**Matthias Trapp, Haik Lorenz, Jürgen Döllner**

*Hasso-Plattner-Institute, University of Potsdam, Prof.-Dr.-Helmert-Str. 2-3, Potsdam, Germany  
{matthias.trapp | haik.lorenz | juergen.doellner}@hpi.uni-potsdam.de*

**Keywords:** Stereoscopic Imaging, Non-planar projections, Real-time rendering

**Abstract:** Stereo rendering, as an additional visual cue for humans, is an important method to increase the immersion into 3D virtual environments. Stereo pairs synthesized for the left and right eye are displayed in a way that the human visual system interprets as 3D perception. Stereoscopy is an emerging field in cinematography and gaming. While generating stereo images is well known for standard projections, the implementation of stereoscopic viewing for interactive non-planar single-center projections, such as cylindrical and spherical projections, is still a challenge. This paper presents the results of adapting an existing image-based approach for generating interactive stereoscopic non-planar projections for polygonal scenes on consumer graphics hardware. In particular, it introduces a rendering technique for generating image-based, non-planar stereo pairs within a single rendering pass. Further, this paper presents a comparison between the image-based and a geometry-based approach with respect to selected criteria.

## 1 INTRODUCTION

Stereoscopy is the phenomenon of simultaneous vision with two eyes, producing a perception of the relative distances between objects in space. Stereoscopy can be created by using a stereo image pair displayed with active or passive stereo viewing concepts, which enable the experience of the stereo sensation. This feature is a requirement for 3D immersive digital environments. Creating stereo image pairs is straightforward for planar projections that can be accelerated by graphics hardware. The renderer needs to create an image pair, one image for the left eye and one for the right eye. Most of today's computer games and visualization frameworks offer a 3D stereo mode for standard planar projections.

Enabling interactive stereo rendering for non-planar projections is not a trivial problem. This is especially true for rendering on polygonal consumer graphics hardware without the support of parallel or distributed systems. The optimal solution for this problem enfold the following attributes: It should enable rendering at interactive frame rates for large-scale models, such as virtual 3D city models or land-

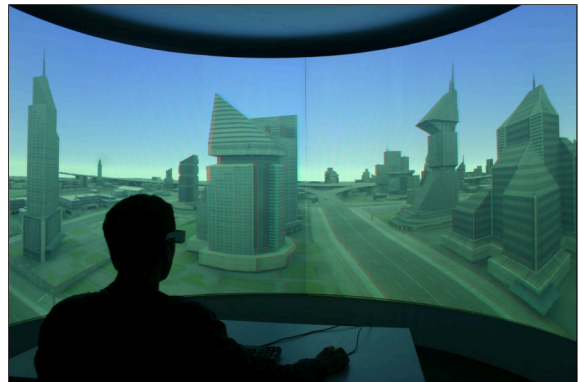


Figure 1: Application of a passive stereo rendering technique for immersive virtual environments.

scapes on current consumer hardware. Further, the approach should be applicable to multiple variants of single-center projections, support omni-directional stereo, deliver high-quality images, and should be easy to implement and integrate into existing rendering frameworks. Figure 1 shows a passive anaglyph stereo rendering of a 180° cylindrical projection performed in real-time, displayed on a half-cylindrical screen.

This paper presents the application of image-based (IBA) and geometry-based (GBA) approaches for creating non-planar projections (NPP) to stereo rendering, and makes the following contributions to the reader: It extends an image-based approach for generating non-planar projection described in (Trapp and Döllner, 2008) with the functionality of interactive rendering for active and passive stereo viewing. We present a new rendering technique that renders these stereo images within a single scene rendering pass. The paper gives explanations for the implementation using modern graphics hardware. We further present a performance evaluation of the extended rendering technique as well as a comparison between IBA and GBA described in (Lorenz and Döllner, 2008) by using different criteria.

This paper is structured as follows. Section 2 gives an overview of related and previous work concerning our topic. Section 3 introduces the basic concepts of stereoscopic rendering and reviews the image-based and geometry-based approaches for generating non-planar projections. Section 4 focuses on the implementation of our rendering technique and presents a performance evaluation. Section 5 compares IBA and GBA. Section 6 discusses the results and concludes the paper.

## 2 RELATED & PREVIOUS WORK

Besides approaches for omni-directional non-planar projections and camera systems (Peleg et al., 2001) that stitch real-world images to obtain a still stereo image, we find approaches for stereo rendering on multi-projector systems (Bimber et al., 2005). This work reflects non-planar projections for single projection centers which can be created using *image-based* and *geometry-based* approaches. We focus on the last two.

**Image-based Approaches** These rendering techniques are mainly based on two phases. First, a raster representation of the virtual scene is created using off-screen rendering. In the second phase, this representation is used to create different projections or image-distortions using image warping in a post processing step (Yang et al., 2005). In (Trapp and Döllner, 2008) a generalization of this approach is described that uses a cube map texture to represent the virtual environment and create multiple NPPs and variants of image distortions.

**Geometry-based Approaches** A straight-forward GBA implementation simply projects all mesh ver-

tices non-planarly and rasterizes the primitives immediately (Spindler et al., 2006). The inadequate linear interpolation during rasterization requires highly tessellated meshes for artifact-free renderings. Dynamic mesh tessellation based on instancing (Boubekeur and Schlick, 2008; Tatarinov, 2008), geometry shaders (Lorenz and Döllner, 2008), or hardware tessellation units (Tatarchuk, 2007) can ensure this property for arbitrary meshes. An alternative approach is tessellating the non-planar projection into smaller and simpler projections. (Hou et al., 2006) describes an approach for rendering arbitrary projections which is conceptually based on beam tracing.

## 3 BASIC CONCEPTS

Regardless of the rendering techniques used for creating non-planar projections, the creation of stereoscopic views comprises the following two basic steps:

1. **Generating Stereo Pairs:** The NPP for the left and right images are synthesized by using image-based or geometry-based rendering techniques.
2. **Stereo Rendering:** The stereo pairs are combined into a single frame buffer (passive stereo) or rendered into two frame buffers (active stereo) by using post-processing compositing passes.

### 3.1 Image-based Projections

Before we describe how to create stereo renderings for non-planar projections, we briefly review the approach described in (Trapp and Döllner, 2008). This approach uses a dynamically created cube-map texture to capture the complete virtual environment that surrounds the virtual scene camera. The non-planar projections are derived by applying a projection function  $\delta_p$  that samples the cube map using computed normal vectors. This functionality is implemented in a fragment shader program using a post-processing pass. It is activated when rendering a screen-aligned quad that covers the whole view port.

This paper adapts and extends the described concept to support stereo rendering. A naïve approach is the creation of two cube maps using two rendering passes and then perform stereo rendering by computing two non-planar projections. To avoid unnecessary state changes for multi-pass rendering, we propose a method that creates two cube map textures within a single rendering pass. This fully hardware-accelerated technique is described in Section 4. It integrates into the referenced image-based approach, and therefore benefits from further functionality such as generalizations of non-planar projections.

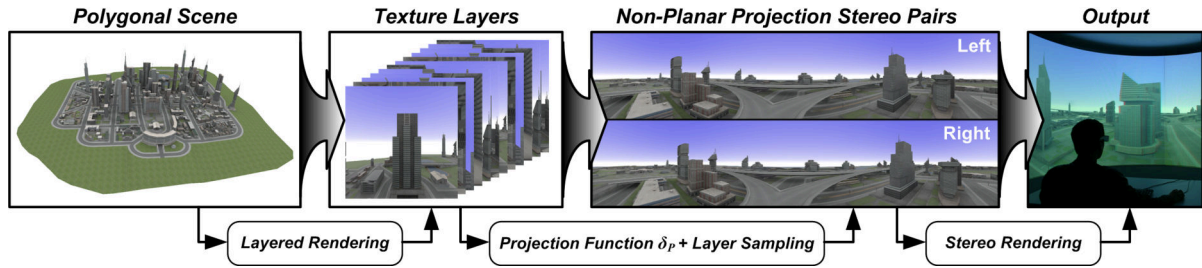


Figure 2: Overview of the implementation concept for image-based stereo rendering for non-planar projections. Layered rendering is used to create image representations of the input geometry. These images are synthesized into stereo pairs of non-planar projections which are then viewed in stereo.

### 3.2 Geometry-based Projections

Object-space approaches do not rely on resampling of an intermediate texture to achieve the non-planar projection effect. They apply the projection directly to mesh vertices and render the final image immediately using regular rasterization. At this point, we summarize the approach taken by (Lorenz and Döllner, 2008). They use geometry shaders to generate a view-dependent tessellation with limited edge length per primitive. For performance, they rely on an intermediate mesh using barycentric coordinates. Since geometry shaders are currently not capable of emitting sufficient primitives at once, a three-pass scheme is used: first, the required tessellation level is determined per original primitive. Second, the existing tessellated intermediate mesh is refined to meet the new tessellation requirements. Third, the intermediate mesh is converted into a fully attributed mesh, projected, and rendered to the screen.

To enable stereo rendering, layered rendering can be used to create both images at once. The third pass simply emits each primitive twice using separate projections and directs them into two different layers. A subsequent compositing pass creates the stereo view.

## 4 IMPLEMENTATION

Our exemplary implementation is based on OpenGL (NVIDIA, 2008) and the OpenGL shading language (Kessenich, 2006). The GBA enables the direct output of the stereo pair using a single scene evaluation and is not discussed furthermore. This section focuses on the extension of the IBA to create the raster representation within a single scene rendering pass. Figure 2 shows an overview of our implementation concept. The rendering process for creating stereo pairs enfolds the following three steps per frame:

1. **Update Camera Orientation:** The twelve camera orientations for all cube-map faces are updated using the parallel camera mode. The off-axis and

toe-in camera modes (Bourke and Morse, 2007) are not used, since they lead to artifacts or missing stereo disparity.

2. **Create Raster Representations:** There are three alternatives for creating raster representation of the virtual 3D scene. The first uses multi-pass rendering to create two cube-map textures by rendering one pass for each cube map face, i.e., twelve passes in total. The second requires one pass for each cube-map texture by using *render-to-cubemap* (RTC), i.e., two passes in total. The third creates twelve layers, corresponding to each face of two cube maps textures, within a single rendering pass. This section focuses on the third alternative.
3. **Apply Projection:** The raster representations are transformed into two non-planar projections (left, right). This is done in one or two full-screen post-processing passes using a single frame buffer for passive stereo rendering or a dual frame buffer for active hardware stereo rendering.

### 4.1 Creating Raster Representations

The present generation of raster-based polygonal rendering hardware (Blythe, 2006) enables the application of *layered rendering* or RTC. Using the support of geometry amplification, there are two possibilities to create a raster representation of the virtual scene: render to twelve layers interpreted as faces of two cube-map textures or render to six layers interpreted as a single cube-map texture with two render targets by using *multiple render-targets* (MRT). Currently, there is a lack of support for multiple depth buffers. Thus, using MRT is not possible because both targets would share the same depth buffer. This would lead to incorrect rendering results.

However, the first approach requires the binding of two cube map textures to a frame buffer object. Unfortunately, this is not possible due to API restrictions (OpenGL and Direct3D). Therefore, we perform rendering to twelve 2D texture layers and interpret them

```

#version 120
#extension EXT_geometry_shader4 : enable
uniform mat4 VPM[12]; //View projection matrices

bool cullViewFrustum(in vec4 P[3]) {
    const vec4 plane = vec4(-1.0, -1.0, 1.0, 1.0);
    vec4 T[3];
    T[0] = clamp(P[0].xyxy * plane - P[0].w, 0.0, 1.0);
    T[1] = clamp(P[1].xyxy * plane - P[1].w, 0.0, 1.0);
    T[2] = clamp(P[2].xyxy * plane - P[2].w, 0.0, 1.0);
    return !any(notEqual(T[0]*T[1]*T[2], vec4(0.0)));
}

bool cullBackFace(in vec4 P[3]) {
    vec2 d0 = P[1].xy * P[0].w - P[0].xy * P[1].w;
    vec2 d1 = P[2].xy * P[0].w - P[0].xy * P[2].w;
    float w = min(min(P[0].w, P[1].w), P[2].w);

    return d1.x * d0.y < d0.x * d1.y || w <= 0.0;
}

void main(void) {
    for(int face = 0; face < 12; ++face) {
        gl_Layer = face; //Assign layer ID
        vec4 P[3]; //Compute screen coordinates
        P[0] = VPM[face] * gl_PositionIn[0];
        P[1] = VPM[face] * gl_PositionIn[1];
        P[2] = VPM[face] * gl_PositionIn[2];
        //Perfrom culling algorithms
        if(cullViewFrustum(P) && cullBackFace(P)) {
            for (int i = 0; i < 3; i++) {
                gl_Position = P[i];
                //Fill further interpolants
                EmitVertex();
            } //endfor
            EndPrimitive();
        } //endif
    } //endfor
}

```

Figure 3: OpenGL geometry shader implementation of layered rendering.

as two cube map textures. The texture layers are organized within a single 3D texture or 2D texture array.

## 4.2 Shader-based Implementation

To implement the layered-rendering technique, we use OpenGL with extensions (NVIDIA, 2008) and geometry shader functionality. A geometry shader duplicates and emits triangles which are transformed into the camera-coordinate system of the respective cube map face and are then projected. Therefore, we calculate the view-projection transformation matrices and bind them as shader constants. A layer ID (0-11) is assigned to every emitted triangle. It defines the target layer of the framebuffer object. The geometry shader shown in Figure 3 implements the main logic of our concept. Since a triangle can only be visible in at most five cube map faces, we can limit the maximum primitive output to 30 triangles. Further, the geometry shader uses a conservative view-frustum culling (`cullViewFrustum`) and back-face culling (`cullBackFace`) (Persson, 2007).

## 4.3 Layer Sampling

After texture-layer creation, there are two different ways to emulate the cube-map texture. Copying the 2D layers into two cube-map textures introduces un-

necessary state changes per frame. As alternative, we chose to re-implement cube map texture sampling in a fragment shader program. The sampling algorithm consists of two parts: *face selection* that maps the cube face intersected by the normal to the layer number of the texture array and the 2D *texture coordinate generation*. There are mainly two ways to implement such algorithm within a fragment shader program:

- Analytic Sampling Approach (ASA): Sampling can be implemented via cube-ray intersection or using dynamic branching to determine faces without additional data structures.
- Reference Sampling Approach (RSA): Instead of performing ASA computation per sample, we can derive the faces and sampling coordinates by encoding the cube map face IDs and 2D texture coordinates into a *reference cube-map texture* (RCT). This texture is created in a preprocessing step and uses a 32bit floating-point format for high-precision sampling, and also to avoid value clamping of the face IDs.

The ASA implementation requires 54 arithmetic logic unit (ALU) instructions while the RSA needs only four. RSA without mip-mapped cube map texture introduces sampling artifacts at the borders of the RCT. To minimize these artifacts, the resolution of the reference cube map should be the same as for the texture layers. This adds additional memory requirements. Conducted performance measurements show only a small difference between both techniques (average of < 0.02 FPS on a NVIDIA GeForce GTX 280). According to the reasons above, we chose to use ASA over RSA.

## 4.4 Stereo Rendering

After the NPP for the left and right eye are created, the rendering technique has to perform the image synthesis for stereo viewing:

- Rendering for Passive Stereo: Passive stereo viewing is independent of the refresh rates of the output device and can be achieved by using mainly two methods: anaglyph or polarized rendering. Anaglyph images provide a stereoscopic 3D effect when viewed with two colored glasses, each with a chromatically opposite color (usually red and cyan). This can be implemented by computing two projections and performing a full-screen compositing pass. Another possibility is the use of polarized screens or projector filters in combination with polarized glasses.
- Rendering for Active Stereo: Frame-sequential, active stereo can be achieved by using shutter

glasses that are synchronized with the graphics hardware. Here, alternate left and right images are displayed on the screen, multiplexed in time. Active stereo can be implemented using OpenGL and a quad buffer. Similar to polarized rendering, it requires the evaluation of the projection function twice.

## 4.5 Performance Evaluation

The performance tests are conducted on two different platforms: NVIDIA GeForce 8800 GTS GPU with 640MB video RAM on an AthlonTM64 X2 Dual Core 4200+ with 2.21 GHz, 2 GB of main memory, as well as NVIDIA GeForce GTX 280 with 1024 MB video RAM on a Intel Core2 Duo, 3 GHz 3,25 GB of main memory. Table 1 shows a comparison of the two different cube map creation alternatives described in Section 4.1 with respect to the number of input triangles. Each test comprises the creation of two cube maps or one texture array with  $1024^2$  pixel texture resolution and the rendering of a horizontal  $360^\circ$  cylindrical projection with a view port size of  $2048 \times 768$  pixels using anaglyph stereo viewing. No cube map face culling techniques were used.

Table 1: Performance comparison of image-based rendering for creating anaglyph stereoscopic views. The measurements (FPS) are taken for a  $360^\circ$  cylindrical projection with anaglyph passive stereo and a view port resolution of  $2048 \times 768$  pixels.

Triangles	Passes	8800 GTS	GTX 280
34,596	2	6.01	20.93
	1	6.37	29.23
236,276	2	0.80	7.82
	1	0.84	8.95
540,655	2	0.57	3.57
	1	0.39	4.13
3,210,162	2	0.11	0.45
	1	0.09	0.60

## 5 COMPARISON

We compare the geometry-based and image-based approaches with respect to the following criteria:

**Stereo Functionality:** The image-based approach is limited to generating directional panoramic views because the raster representations are created with a fixed base line for each camera orientation. Following to that, the angle disparity is zero for views along the base-line and the user observes only depth disparity.

Table 2: Performance comparison between the image-based and geometry-based approach for generating stereo images pairs. The measurements (FPS) are taken for a  $180^\circ$  panoramic view with anaglyph passive stereo and a view port resolution of  $1280 \times 1024$  pixels.

Triangles	IBA		GBA	
	GTS	GTX	GTS	GTX
34,596	20.66	42.55	31.32	52.15
236,276	6.04	24.51	12.42	35.77
540,655	2.58	9.40	3.49	9.11
3,210,162	0.41	2.83	0.93	4.14

However, the geometry-based approach is able to create full  $360^\circ$  omni-directional stereo panorama. The IBA is limited to the parallel camera mode to avoid artifacts in the stereo pairs. Thus, the GBA has a clear advantage over the IBA.

**Rendering Performance:** Table 2 shows a comparison between IBA and GBA with respect to the number of input primitives. Both rendering techniques require only a single scene rendering pass for passive stereo viewing of a single cylindrical projection with a horizontal FOV of  $180^\circ$  and a vertical FOV of  $90^\circ$ . The IBA uses cube map face culling to render only necessary faces. The measurement shows that the GBA performs better than the IBA for low to medium model complexity. For a higher model complexity, both approaches obtain similar non-real-time performance, but the GBA is still faster. In the most common case of rendering a single NPP, GBA should be preferred over the IBA.

**Image Quality:** The major drawback of the IBA is image-quality. In contrast to GBA, sampling artifacts are introduced while creating the projections. This is especially problematic for wire-frame renderings or NPR techniques such as hatching or similar. Figure 4 shows the advantage of GBA over IBA.

**Memory Footprint:** A further criteria considers the memory footprint for data related to the rendering

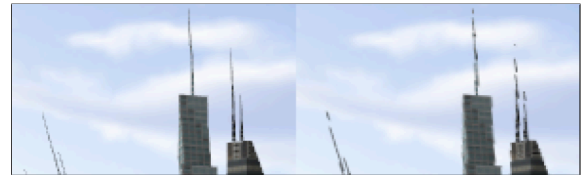


Figure 4: Comparison of the image quality between the geometry-based (left) and image-based approach (right). The screen shots are conducted using a cube map texture of  $2048^2$  pixels on a target resolution of  $1600 \times 1200$  pixels.



technique, e.g., texture size and geometry. This is an important criteria for applications that use out-of-core rendering mechanisms. The footprint of the IBA can be considered constant. It depends on the texture resolution  $s$ , the precision per color channel  $b$ , the number of color channels  $c$ , and the number of raster layers  $l$ . The footprint can be approximated by:  $O_{IBA}(l, s, b, c) = 2 \cdot l \cdot c \cdot b \cdot s^2$  byte without mip-maps. This parametrization enables the user to balance the trade-off between image quality and memory consumptions, as well as the runtime complexity.

The memory footprint of the GBA is dynamically view-dependent and scales linearly with the number of input triangles  $t$ . Further, memory footprint depends on the average rate of primitive amplification  $r$  (for a  $180^\circ$  cylindrical projection  $r = 1.5 - 2$ ), and the size of each triangle in an intermediate data structure  $i = 16$  byte. The amount of additional memory can be approximated by:  $O_{GBA}(t, r, i) = t \cdot r \cdot i$ . Following to that, the space complexity of the GBA is independent of rendering a single NPP or a stereo pair of NPP. For the complex model (3,210,162 triangles) the additional memory requirement for a  $180^\circ$  panorama projection is  $O_{GBA} \approx 69$  MB. This corresponds to four RGBA raster layers with  $1024^2$  pixels resolution. For a higher FOV:  $O_{GBA} < O_{IBA}$  is valid in any case.

## 6 CONCLUSIONS

This paper presents an overview for creating stereo renderings of non-planar projections with image-based and geometry-based rendering techniques. In particular, it describes the implementation of a single-pass image-base rendering technique as an extension to an existing framework. We evaluate the performance of this technique with respect to the number of input triangles. We further present a comparison between geometry-based and image-based approaches for generating stereo pairs with respect to of four different criteria.

This comparison shows that both approaches are capable of rendering stereographic non-planar projections. The GBA is predominant over IBA in the range of functionality with respects to stereo rendering, the quality of the output images, as well as the rendering performance. The IBA has advantages considering the constant space and low implementation complexity. A disadvantage of both rendering techniques is the limitation to polygonal scenes only. They cannot be applied directly to volume rendering without major changes.

Following to these results, we consider the GBA more suitable for stereo rendering of non-planar pro-

jections than the IBA. According to our performance measurements, both approaches achieve satisfying results for 3D scenes of the medium complexity (500,000 triangles).

## REFERENCES

- Bimber, O., Wetzstein, G., Emmerling, A., and Nitschke, C. (2005). Enabling View-Dependent Stereoscopic Projection in Real Environments. In *IEEE ISMAR '05*, pages 14–23, Washington, DC, USA. IEEE Computer Society.
- Blythe, D. (2006). The Direct3D 10 System. In *SIGGRAPH '06: ACM SIGGRAPH 2006 Papers*, pages 724–734, New York, NY, USA. ACM Press.
- Boubekeur, T. and Schlick, C. (2008). A Flexible Kernel for Adaptive Mesh Refinement on GPU. *Computer Graphics Forum*, 27(1):102–114.
- Bourke, P. D. and Morse, P. (2007). Stereoscopy, Theory and Practice. Workshop, VSMM 2007, Brisbane.
- Hou, X., Wei, L.-Y., Shum, H.-Y., and Guo, B. (2006). Real-time Multi-Perspective Rendering on Graphics Hardware. In *EUROGRAPHICS Symposium on Rendering*. Blackwell Publishing.
- Kessenich, J. (2006). *The OpenGL Shading Language Language Version: 1.20 Document Revision: 8*.
- Lorenz, H. and Döllner, J. (2008). Dynamic Mesh Refinement on GPU using Geometry Shaders. In *Proceedings of the 16-th WCSG 2008*.
- NVIDIA (2008). *NVIDIA OpenGL Extension Specifications for the GeForce 8 Series Architecture (G8x)*. NVIDIA.
- Peleg, S., Ben-Ezra, M., and Pritch, Y. (2001). Omnistereo: Panoramic Stereo Imaging. *IEEE Transactions on Pattern Analysis and Machine Intelligence*, 23(3):279–290.
- Persson, E. (2007). *ATI Radeon HD 2000 Programming Guide*. AMD Graphics Products Group.
- Spindler, M., Bubke, M., Germer, T., and Strothotte, T. (2006). Camera Textures. In *Proceedings of the 4th GRAPHITE*, pages 295–302. ACM.
- Tatarchuk, N. (2007). Real-Time Tessellation on GPU. In *Course 28: Advanced Real-Time Rendering in 3D Graphics and Games. ACM SIGGRAPH 2007*.
- Tatarinov, A. (2008). Instanced Tessellation in DirectX10. In *GDC '08: Game Developers' Conference 2008*.
- Trapp, M. and Döllner, J. (2008). A Generalization Approach for 3D Viewing Deformations of Single-Center Projections. In José Braz, N. J. N. and Pereira, J. M., editors, *GRAPP 2008*, number 3, pages 162–170. INSTICC Press.
- Yang, Y., Chen, J. X., and Beheshti, M. (2005). Nonlinear Perspective Projections and Magic Lenses: 3D View Deformation. *IEEE Computer Graphics and Applications*, pages 76–84.